



First triclosan-based macrocyclic inhibitors of InhA enzyme

Frédéric Rodriguez^{a,*}, Nathalie Saffon^b, José Camilla Sammartino^c, Giulia Degiacomi^c,
Maria Rosalia Pasca^c, Christian Lherbet^{a,*}

^a LSPCMIB, UMR-CNRS 5068, Université Paul Sabatier-Toulouse III, 118 Route de Narbonne, 31062 Toulouse Cedex 9, France

^b Institut de Chimie de Toulouse, FR2599, 118 Route de Narbonne, 31062 Toulouse, France

^c Dipartimento di Biologia e Biotecnologie "Lazzaro Spallanzani", Via Ferrara 9, 27100 Pavia, Italy

ARTICLE INFO

Keywords:

Macrocycle
Triclosan
Enoyl-ACP-reductase
InhA
Mycobacterium tuberculosis
Marchantin analogue

ABSTRACT

Two macrocyclic derivatives based on the triclosan frame were designed and synthesized as inhibitors of *Mycobacterium tuberculosis* InhA enzyme. One of the two molecules **M02** displayed promising inhibitory activity against InhA enzyme with an IC₅₀ of 4.7 μM. Molecular docking studies of these two compounds were performed and confirmed that **M02** was more efficient as inhibitor of InhA activity. These molecules are the first macrocyclic direct inhibitors of InhA enzyme able to bind into the substrate pocket. Furthermore, these biaryl ether compounds exhibited antitubercular activities comparable to that of triclosan against *M. tuberculosis* H37Rv strain.

1. Introduction

Tuberculosis (TB) is a scourge and one of the top 10 causes of death and the leading cause from a single infectious agent worldwide [1]. In 2017, 1.6 million TB deaths including about 300,000 deaths among HIV-positive people were estimated. Even if the TB incidence is falling at about 2% per year, the number of TB infected people remain high. With the emergence of multidrug-resistant (MDR) and extensively drug-resistant (XDR) *Mycobacterium tuberculosis* (*Mtb*) strains, there is an urgent need to discover new drugs [2,3]. Enzymes involved in the biosynthesis of mycolic acids represent the main cellular targets, in particular proteins belonging to the Fatty Acid Synthesis (FASII) system, which is not present in humans [4]. One of them, InhA enzyme, essential for *Mtb* survival [5], catalyzes the reduction of the NADH-dependent stereospecific reduction of 2-*trans*-enoyl-ACP (acyl-carrier-protein) [6]. The current anti-TB front-line drug, isoniazid (INH) is one of the most efficient compound to treat TB and inhibits indirectly InhA. Indeed, INH acts as a prodrug requiring an oxidative activation by KatG, a catalase-peroxidase to generate the isonicotinoyl radical. This radical species covalently reacts with NAD resulting in an isonicotinoyl-NADH adduct (INH-NADH), acting as the real inhibitor of InhA enzyme [7,8]. Different classes of direct inhibitors of InhA enzyme were investigated such as Triclosan (TCL, Fig. 1B) [9,10] and derivatives, GEQ analogues [11–14], triazoles [15] or thiazoles [16]. Surprisingly, little attention has been paid to macrocyclic InhA inhibitors although the active site of InhA is large and buried deeply. It can accommodate the cofactor NADH and also the long fatty

acid intermediates [17]. Taking advantage of this large binding site, pyridomycin [18] produced by *Streptomyces pyridomyceticus* [19] is the sole macrocyclic inhibitor of InhA enzyme (Fig. 2A). This natural product acts as a competitive inhibitor at both the lipid substrate- and NADH cofactor-binding pockets of InhA.

In 2003, Kuo et al. reported the X-ray structure (1P45) of two molecules of Triclosan in the binding site of InhA enzyme (Fig. 2) [13]. Based on this structure, we decided to design macrocyclic inhibitors of InhA, involving two molecules of triclosan, as an alternative approach compared to those existing for analogues of triclosan as inhibitors of InhA (Fig. 2). These new TCL-based macrocyclic molecules represent regioisomer analogues of macrocyclic molecules such as riccardins, neomarchantins or isomarchantins, member of the macrocyclic bis(bi-benzyl) natural products (Fig. 1B) [20]. It is noteworthy that these natural bisbenzyl products exhibit broad biological activities; in fact, they are anticancers [21,22], antibacterials [23,24] or antifungals [25].

In this work, we reported the design, the synthesis and the biological evaluation of two macrocyclic biaryl-ether-based molecules, inspired from TCL, as inhibitors of InhA enzyme and as antitubercular agents.

2. Results and discussion

2.1. Design of the macrocyclic inhibitors

In 2003, unexpectedly, two triclosan molecules were found in the substrate binding site of InhA enzyme [13]. One molecule of triclosan

* Corresponding authors.

E-mail addresses: build@chimie.ups-tlse.fr (F. Rodriguez), lherbet@chimie.ups-tlse.fr (C. Lherbet).

<https://doi.org/10.1016/j.bioorg.2019.103498>

Received 14 October 2019; Received in revised form 2 December 2019; Accepted 5 December 2019

Available online 06 December 2019

0045-2068/ © 2019 Elsevier Inc. All rights reserved.

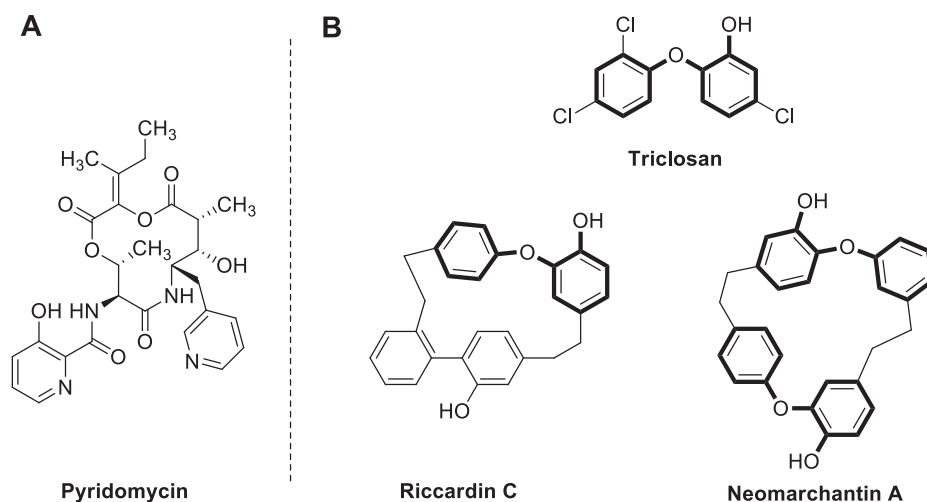
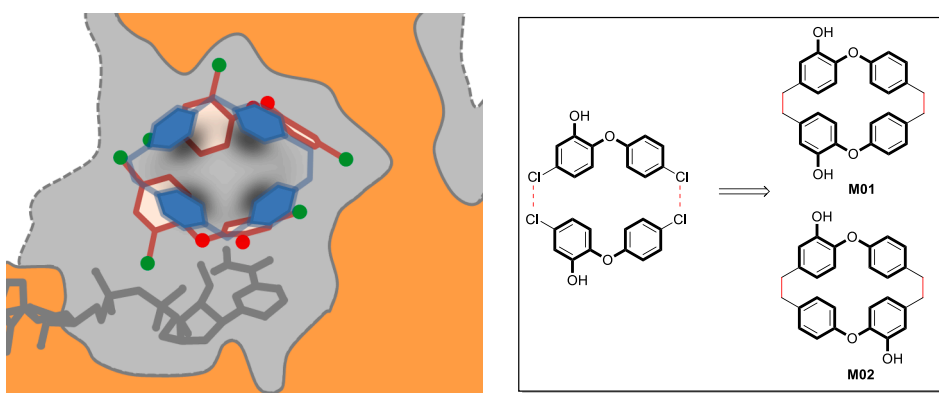


Fig. 1. A: Pyridomycin, a macrocyclic inhibitor of InhA enzyme. B: Triclosan and examples of macrocyclic biarylethers: Riccardin C and Neomarchantin A.



occupies the same space as the substrate. The phenol ring forms a stacking interaction with NADH and his hydrogen bonded to the phenolic group of Tyr158. The second molecule of triclosan is found in chain A of the structure 1P45 and binds at the position of the aliphatic part of the substrate analogue THT in an almost entirely hydrophobic area. The two hydroxyl groups on each triclosan are not oriented in the same way. Based on the structure reported by Kuo et al. [13], Fig. 2 shows that simple metrics such as distances between atoms could provide informations on the predisposition of the molecules toward macrocyclic compounds. In our case, chloride atoms bind in close proximity to each other and could be replaced by methylene groups. Consequently, two candidates, i.e. macrocycles **M01** or **M02**, have been selected as potential macrocyclic inhibitors of InhA enzyme. As for these designed molecules, marchantins and analogues have the particularity to possess two methylene groups as linkers between each biaryl moiety.

2.1.1. Synthesis of the precursors 4, 5 and 7

Different methods were developed to synthesize macrocyclic bis-benzyl-based molecules such as riccardins, marchantins, neomarchantins or isomarchantins [20]. Not surprisingly, the most difficult step is the macrocyclization step. Just by looking at the precedent synthesis of the aforementioned compounds, the most reliable macrocyclisation step was realized through Wittig olefination or related methodologies, followed by hydrogenation of the double bond. This strategy has been recently illustrated by the contributions of the groups of Lou [26] and Miyachi [27].

On this basis, the initial steps started by the synthesis of the precursors 4, 9 and 12 that will be used for the Wittig olefination. Vanillin was initially converted to its acetal 3, as described. The resulting phenol was condensed with either 4-fluorobenzaldehyde either methyl 4-

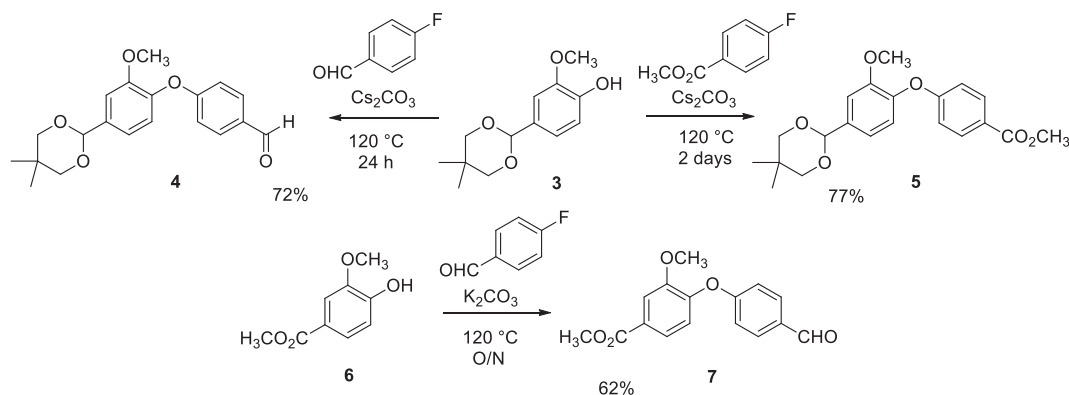
formylbenzoate to afford biaryl ethers 4 and 5. In a same way, biaryl ether 7 was synthesized from the commercially available phenol 6 (see Scheme 1).

Aldehyde 7 was reduced to its corresponding alcohol derivative 8 by NaBH_4 and treated with triphenylphosphine hydrobromide (Fig. 4). The same protocol was used for compound 5 to afford compound 12, except that acetal derivative 5 was previously deprotected in the presence of PPTS (Scheme 2).

2.1.2. Synthesis of the macrocycles

The general procedures for the synthesis of the two macrocycles are outlined in Schemes 3 and 4.

The union of intermediates 9 and 12 with compound 4 was accomplished using Wittig reaction to afford the corresponding stilbene intermediates that were subsequently hydrogenated to give compounds 13 and 18. Then, these compounds were reduced by LiAlH_4 and PPTS treatment provided the two aldehydes 15 and 20. Reactions with triphenyl phosphine hydrobromide furnished compounds 16 and 21 in very good yields. Macrocyclic compounds 17 and 22 were synthesized in two steps from 16 and 21, respectively. Firstly, compounds 16 and 21 were cyclized via an intramolecular Wittig reaction between a biaryl-ether aldehyde and a phosphonium salt, according to a reported method [26]. Then the stilbene intermediates were reduced by hydrogenation to afford compounds 17 and 22. Double demethylation of compounds 17 and 22 by BBr_3 at low temperature gave desired compounds **M01** and **M02** in good yield. The structure of compound **M01** was confirmed through X-ray crystallography (Fig. 3; for detailed crystallographic data, see the Supporting Information). Unfortunately, it was not possible to obtain single crystals of **M02**: all attempts to crystallize **M02** led to the formation of a polycrystalline material.



Scheme 1. Synthesis of the intermediates 4, 5 and 7 for the synthesis of the two macrocycles.

2.2. Biological evaluation of the macrocycles and intermediates

The molecules were evaluated as inhibitors of InhA enzyme and *Mycobacterium tuberculosis* H37Rv strains. The inhibitory potencies against InhA enzyme of the two macrocyclic molecules were measured spectrophotometrically, according to a procedure already reported [11]. TCL was used as control. In our assays, macrocycle **M01** showed modest inhibition of InhA activity with 52% inhibition at 50 μM (see Table 1). But, to our delight, macrocycle **M02** was clearly more active than **M01** and showed inhibitory activity with a IC_{50} value of 4.7 μM (see Figs. 1 and 4). MICs to **M01** and **M02** were determined against *Mtb* H37Rv growth; **M01** and **M02** activities were comparable to that found for TCL. Considering an approximative IC_{50} of 0.5 μM for TCL (58% at 0.5 μM) against InhA, **M02** remains 10 times less active than TCL while the same molecule is half as active against mycobacteria. **M01** has the same antitubercular activity as TCL but its lack of inhibition on InhA suggests another target for this compound.

2.3. In silico studies of macrocycles M01 and M02 with InhA enzyme

To better understand the binding mode of these macrocycles into the InhA active site, we performed docking experiment to reveal the possible interactions into the protein.

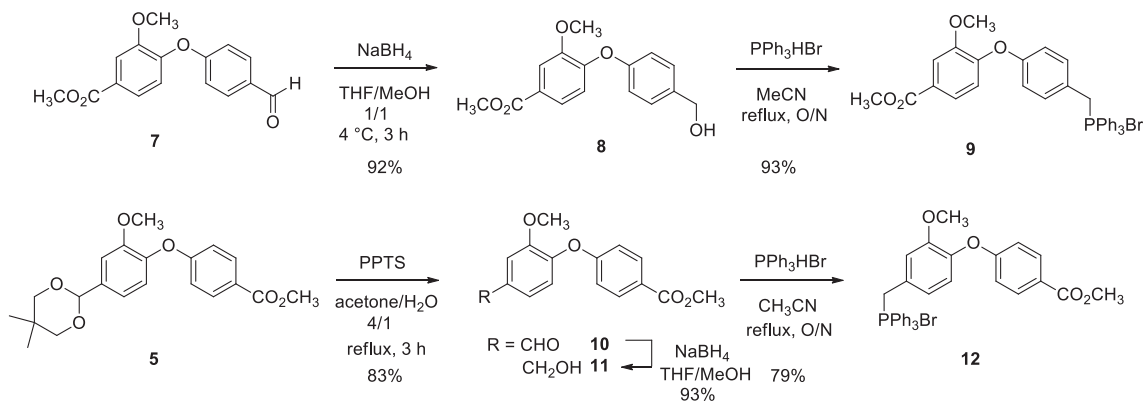
The active site of InhA [7,28] is characterized by a large volume, two variable entries (major and minor portals) at opposite sides of binding cavity, the ability to make structural transitions involving the substrate binding loop (SBL: residues 195–210) and the presence of NAD cofactor interacting with the protein and substrate (or inhibitors). The inhibition schemes include prodrugs that bind to NAD to form an adduct [8,29], direct inhibitors (i.e. some diphenyl ethers derivatives) involved in reversible association with the cofactor [13,30,31], long

time residence inhibitors associated with induced-fit [32–34], or whether the displacement of cofactor [18]. Several keys aspects have emerged among literature, such as the involvement of TYR158, PHE49, the conformation (open or closed states) of helix H6 or the reordering of the SBL loop. But despite classification studies [17,35,36] using different approaches, these different binding and inhibition pathways are not obviously correlated to structure-function relationships (i.e. ligand chemical structures vs. binding site topology) and can be slightly affected by minor changes in ligand structure. All of these elements make docking studies difficult, especially as the best reproduction of crystallographic data by docking methods involves a balance between intermolecular contributions, sometimes antagonist, of ligand-protein and ligand-cofactor interactions.

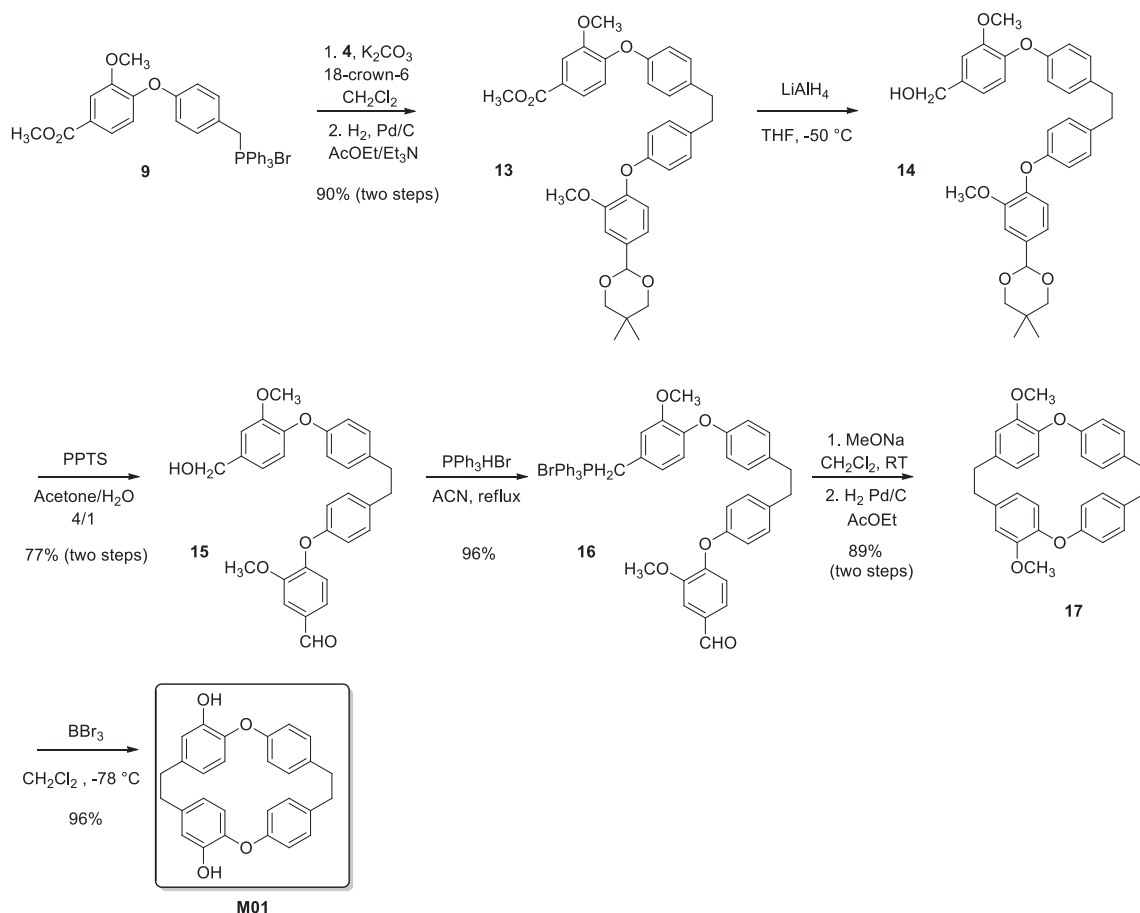
Knowing this intrinsic complexity and the subsequent limitations, docking studies were performed in order to explore the potent insertion of macrocyclic compounds in the binding site of InhA. We used 1P45a (1P45, chain A) [13] as receptor; this structure includes not one but two triclosan (TCL) ligands, interacting upper the cofactor. This arrangement of two triclosan molecules was used as a basis for the design of macrocyclic compounds. We consider also 1P45a as an open structure (relatively to SBL dynamics and major portal, minor portal is closed) able to embed relatively large ligands.

The first result is that **M01** (*cis*) and **M02** (*trans*) molecules are able to dock deeply in the hydrophobic pocket (occupied by most known co-crystallized ligands) near cofactor and TYR158 and can make interactions with both the cofactor and the protein. After docking calculations, most of the poses show that the areas of the hydroxyl and ether groups are positioned along a vertical axis, with one, ether and hydroxyl groups, at the top of the cavity in the hydrophobic pocket and the other at the bottom, close to the cofactor (nicotinamide-ribose part).

In the case of the *cis* compound (**M01**, Fig. 5A and B) the hydroxyl



Scheme 2. Synthesis of the phosphonium bromide intermediates 9 and 12.



Scheme 3. Synthesis of the dimeric macrocyclic triclosan derivative **M01**.

groups are oriented towards the major portal and on the same side than the TYR158 residue. So, interactions with TYR158 and cofactor (2'-OH of ribose) are possible in the case of B1 + topology (see experimental section) by the mean of the bottom hydroxyl group of **M01**. The poses related to A1 topology (see experimental section) have this hydroxyl group too far from TYR158 but interactions with cofactor (nicotinamide) involving ether group are possible.

In the case of the *trans* compound (**M02**, Fig. 5C) the bottom hydroxyl group is headed to the other side and interactions with TYR158 are not possible. But the poses show strong interactions with cofactor (phosphate, ribose) by the mean of this hydroxyl group. The best poses for **M02** display the same A2 topology (see supporting information), a very stable configuration (*N.B.*: this was not the case for **M01**) and give significantly better docking scores and scores contribution (Ligand-Cofactor and Ligand-Protein) than for **M01** compound.

Interestingly, if we compare A topologies (see experimental section) for **M01** and **M02** compounds (Fig. 5D) with C16-fatty acyl substrate (THT, 1BVR [7]) and diaryl ether direct inhibitor such as **PT70** (TCU, 2X22, long time residence inhibitor [32]) we notice that the envelop of **M01** and **M02** is able to share the same chain pathways than these inhibitors in the hydrophobic binding pocket.

Finally, according to score values, interaction patterns and conformational stability (A topology) of poses, the docking experiments show that compound **M02** is more optimized for the binding site than **M01**. These results are in accordance with experimental data; the difference in activity by comparison with triclosan could be correlated with the rigidity of our macrocycles. A longer spacer group i.e. three methylene groups instead of two, would allow for greater flexibility, which could facilitate binding into the substrate binding site.

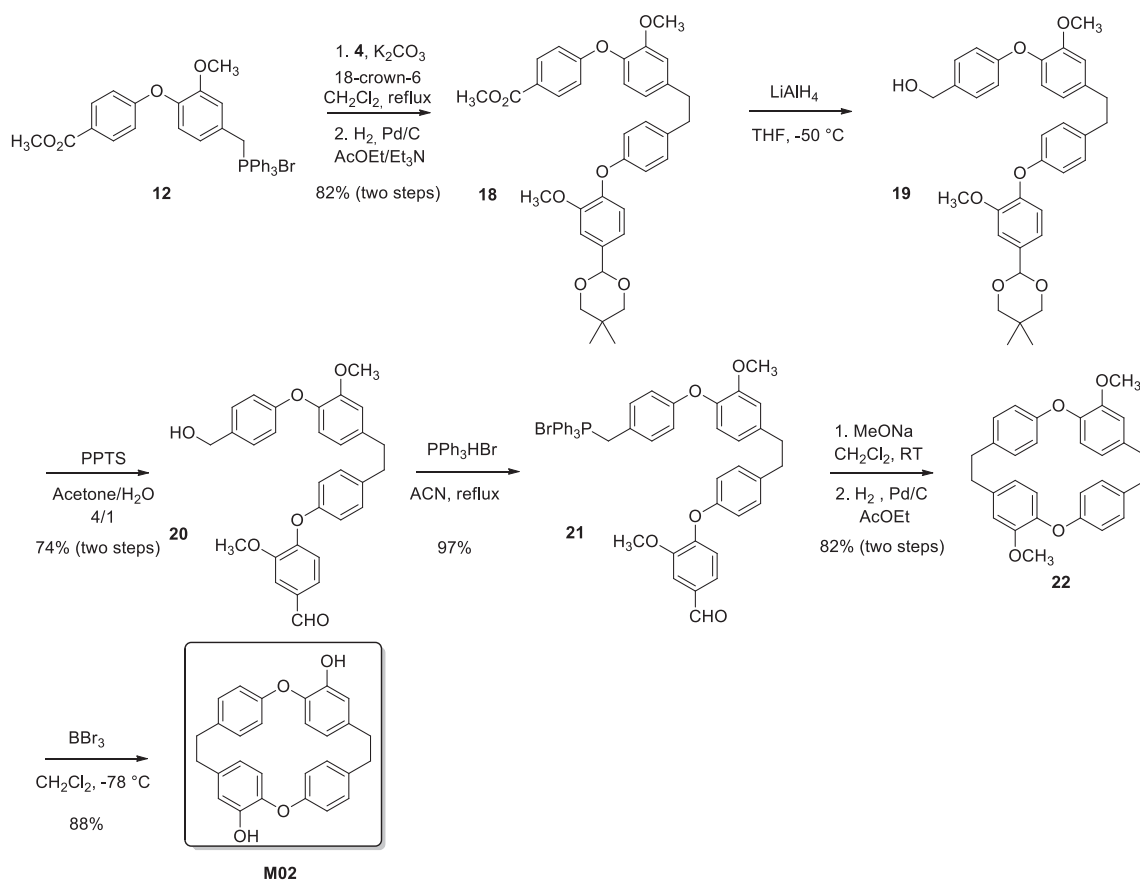
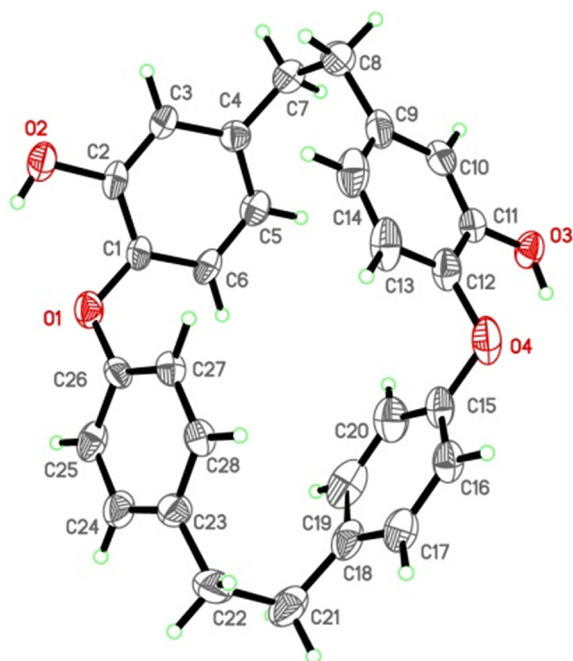
3. Conclusion

In conclusion, two macrocyclic potential inhibitors of InhA enzyme were designed, based on the X-ray structure of the InhA/TCL couple. These two macrocycles incorporating two biaryl compounds were synthesized and the final macrocyclisation step was realized through Wittig olefination. Both molecules were evaluated as inhibitors of InhA enzyme and *Mtb* growth. We found that one of them, macrocycle **M02**, was able to inhibit InhA enzyme with an affinity (IC_{50}) in the micromolar range. Furthermore, molecular docking studies were carried out to understand the difference in bioactivities between both compounds. The results suggest that **M02** binds in the active site. However, in order to increase its enzymatic activity, the molecule could be optimized by considering two approaches: modulating flexibility or modulating substituents on the phenyl moiety (including hydroxyl group and/or chlorine substituents). MIC values for macrocycles **M01** and **M02** were found to be similar to that of TCL. This result is very promising for the upcoming implementation of macrocyclic compounds as direct inhibitors of InhA enzyme.

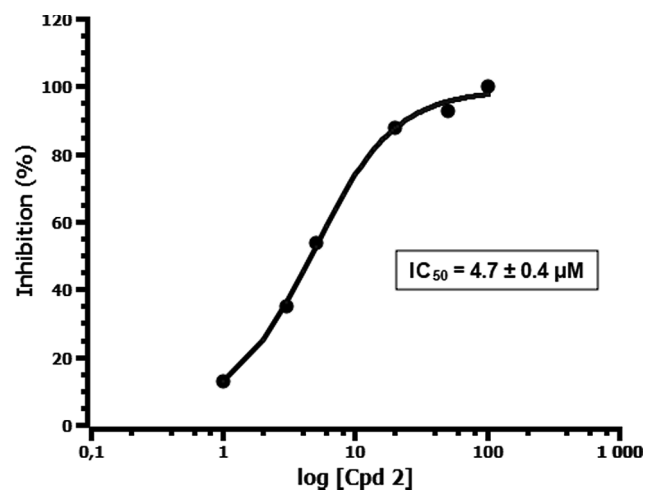
4. Experimental section

4.1. Material and methods

All chemicals were obtained from Aldrich-Sigma, Acros Organics or Alfa Aesar and used without further purification. Anhydrous solvents were freshly distilled before use or were obtained from the M. Braun Solvent Purification System (MB-SPS-800). The melting points were determined on a Mettler Toledo MP50 melting point system and are uncorrected. NMR spectroscopic data were recorded on advance 300

Scheme 4. Synthesis of the dimeric macrocyclic triclosan derivative **M02**.Fig. 3. Molecular view of the X-ray crystal structure of **M01** (Scheme 3), with thermal ellipsoids drawn at the 30% probability level. Only one of the 7 molecules of the asymmetric unit of **M01** is shown and solvent molecules (CH₂Cl₂) are omitted for clarity.Table 1
Activities against InhA enzyme and *Mtb* H37Rv strain.

Compound	% Inhibition at 50 μM (IC ₅₀)	<i>Mtb</i> MIC (μg/mL)
Macrocycle 1 (M01)	52	20
Macrocycle 2 (M02)	93 (4.7 ± 0.4 μM)	40
Triclosan (TCL)	100/58% at 0.5 μM	20
Streptomycin	–	0.25

Fig. 4. Determination of IC₅₀ of macrocycle **M02** against InhA enzyme.

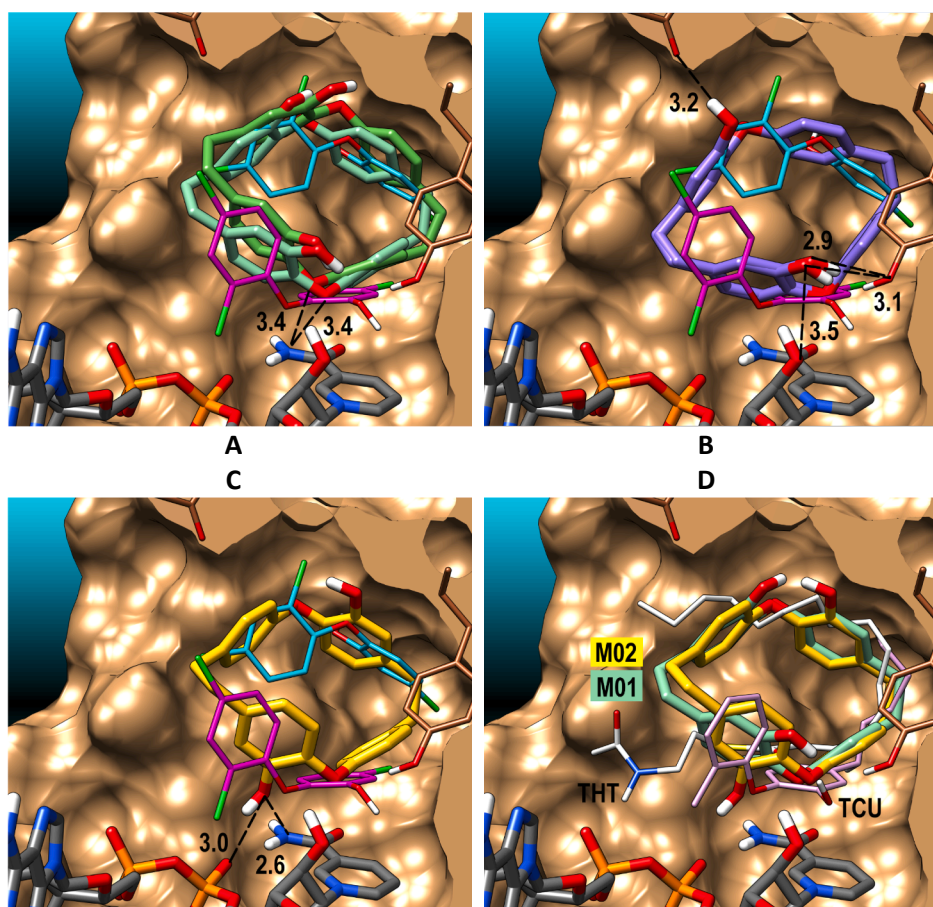


Fig. 5. Docking results showing the four best poses in the case of **M01** (up) and **M02** (down) compounds. The 1P45a (1P45, chain A) structure (brown depicted surfaces) is used, major portal of InhA at left, minor portal at right of the picture. The cofactor NAD (gray) is shown at bottom and the TYR158 and GLN 100 residues (brown) are highlighted. Triclosan molecules, co-crystallized in 1P45 are shown in pink (TCL 500) and cyan (TCL 450). The TCL 500 conformation is known to be typical for many triclosan-based inhibitors. Interatomic distances are expressed in Å (cutoff of 3.5 Å). **A** – Poses {00, 12} for **M01** (green) showing variations of macrocycle topology: type A1. The ether group is interacting (putative hydrogen bond) with the nicotinamid moiety of the cofactor. **B** – Poses {29, 04} for **M01** (purple) for B1+ type topology. The position of hydroxy group in front of the view allows the typical interaction with TYR158 (right). The ligand interacts also with cofactor, additional interaction with GLN100 (up). **C** – Poses {17, 36, 06, 13} for **M02** (yellow) classified with A2 topology. In this case, the hydroxy group engaged in interactions with the cofactor is placed behind the macrocycle. **D** – Comparison of poses {12} for **M01** and {17} for **M02**. The overall topologies (type A) are similar but the position of hydroxy groups are different. The THT compound (substrate, white) from 1BVra [7] and the TCU (inhibitor, light pink) from 2X22a [32] aligned structures are shown.

spectrometer (Bruker, Billerica, MA, USA) operating at 300 MHz for ^1H NMR analysis and 75 MHz for ^{13}C NMR analysis (APT). Chemical shifts (δ) were reported in ppm, using the solvent residual peak as internal reference: CDCl_3 δ = 7.26 ppm/77.0 ppm, MeOD δ = 3.31 ppm/49.0 ppm. spin-spin coupling constants (J) are reported in Hz, while multiplicities are abbreviated by s (singlet), bs (broad singlet), d (doublet), bd (broad doublet), dd (doublet of doublets), t (triplet), td (triplet of doublets), m (multiplet). Mass spectra (DCI/NH $_3$) were obtained on an DSQ ThermoFisher Scientific. For MS–ESI spectra, a Dionex ultimate 3000 UPLC system with a ABSciex Q TRAP 4500 was used. High-resolution mass spectra (HRMS) were recorded on a UPLC Xevo G2 Q-TOF (Waters) or on a GCT Premier (Waters). IR spectra were recorded on a ThermoScientific Nicolet IS50 – ATR diamant from ThermoFisher Scientific. The desired product was purified by flash column chromatography with PuriFlash 430 system using puriFlash® columns from Interchim. The enzymatic evaluation was performed on a Cary Bio 300.

4.1.1. Synthesis of precursors 4, 5 and 7

4.1.1.1. 4-[4-(5,5-Dimethyl-1,3-dioxan-2-yl)-2-methoxyphenoxy]benzaldehyde (4). To a solution of 4-(5,5-dimethyl-1,3-dioxan-2-yl)-2-methoxyphenol (0.485 g, 3.1 mmol) in DMF (20 mL), were added 4-fluorobenzaldehyde (1.1 eq) and cesium carbonate (1.2 eq). The solution was stirred for 24 h at 120 °C under argon. The solvent was removed under reduced pressure. Ethyl acetate was added to the mixture and the mixture solution was washed with water and brine, dried using magnesium sulfate and filtered. The solution was concentrated and the desired product was purified by flash chromatography (linear gradient 95/5 to 60/40 petroleum ether/ethyl acetate) and was isolated as a white powder (0.521 g, 72%). Rf: 0.57 (petroleum ether/ethyl acetate 7/3). Mp: 115–117 °C. $\nu_{\text{max}}/\text{cm}^{-1}$:

2966; 2955; 2864; 1684; 1611; 1596; 1583; 1498; 1396; 1280; 1230; ^1H NMR (300 MHz, CDCl_3) δ 9.88 (s, 1H); 7.78 (m, 2H); 7.22 (d, J = 1.7 Hz, 1H); 7.13 (dd, J = 8.1 Hz, J = 1.7 Hz, 1H); 7.08 (d, J = 8.1 Hz, 1H); 6.96 (m, 2H); 5.40 (s, 1H); 3.80 (s, 3H); 3.70 (m, 2H), 3.64 (m, 2H); 1.31 (s, 3H); 0.81 (s, 3H); ^{13}C NMR (75 MHz, CDCl_3) δ 190.7; 163.4; 151.5; 143.0; 136.9; 131.7; 130.8; 122.2; 119.2; 116.1; 110.7; 101.1; 77.6; 55.8; 30.2; 23.0; 21.8; HRMS (DCI- CH_4) Calculated for $\text{C}_{20}\text{H}_{23}\text{O}_5$ (MH^+): 343.1545. Found: 343.1547.

4.1.1.2. Methyl 4-(4-formyl-2-methoxyphenoxy)benzoate (5). To a solution of 4-(5,5-dimethyl-1,3-dioxan-2-yl)-2-methoxyphenol (0.485 g, 3.1 mmol) in DMF (20 mL), were added methyl 4-fluorobenzoate (1.5 eq) and cesium carbonate (1.5 eq). The solution was stirred for two days at 120 °C under argon. The solvent was removed under reduced pressure. Ethyl acetate was added to the mixture and the mixture solution was washed with water and brine, dried using magnesium sulfate and filtered. The solution was concentrated and the desired product was purified by flash chromatography (linear gradient 95/5 to 70/30 petroleum ether/ethyl acetate) and was isolated as a white powder (0.600 g, 77%). Rf: 0.50 (petroleum ether/ethyl acetate 7/3). Mp: 128–130 °C. $\nu_{\text{max}}/\text{cm}^{-1}$: 2959; 2907; 2870; 1712; 1597; 1502; 1455; 1432; 1410; 1279; 1229; ^1H NMR (300 MHz, CDCl_3) δ 7.94 (m, 2H); 7.21 (d, J = 1.8 Hz, 1H); 7.12 (dd, J = 8.1 Hz, J = 1.8 Hz, 1H); 7.06 (d, J = 8.1 Hz, 1H); 5.40 (s, 1H); 3.87 (s, 3H); 3.81 (s, 3H); 3.79 (m, 2H); 3.67 (m, J = 10.9 Hz, 2H); 1.31 (s, 3H); 0.81 (s, 3H); ^{13}C NMR (75 MHz, CDCl_3) δ 166.6; 162.1; 151.5; 143.6; 136.5; 131.4; 123.9; 122.0; 119.1; 115.7; 110.7; 101.2; 77.7; 55.8; 51.9; 30.2; 23.1; 21.8; HRMS (DCI- CH_4) Calculated for $\text{C}_{21}\text{H}_{25}\text{O}_6$ (MH^+): 373.1651. Found: 373.1643.

4.1.1.3. Methyl 4-(4-formylphenoxy)-3-methoxybenzoate (7). To a

solution of methyl ester derivative **6** (1.5 g, 8.2 mmol) in DMF (30 mL), were added 4-fluorobenzaldehyde (1.2 eq) and potassium carbonate (2 eq). The solution was stirred overnight at 120 °C under argon. The solvent was removed under reduced pressure. Ethyl acetate was added to the mixture and the mixture solution was washed with water and brine, dried using magnesium sulfate and filtered. The solution was concentrated and the desired product was purified by flash chromatography (linear gradient 95/5 to 70/30 petroleum ether/ethyl acetate) and was isolated as a white powder (1.460 g, 62%). Mp: 104–106 °C. $\nu_{\text{max}}/\text{cm}^{-1}$: 2960; 1713; 1698; 1608; 1596; 1584; 1499; 1435; 1297; 1270; 1224; ^1H NMR (300 MHz, CDCl_3) δ 9.91 (s, 1H); 7.82 (m, 2H); 7.70 (s, 1H); 7.68 (m, 1H); 7.08 (m, 1H); 7.01 (m, 2H); 3.92 (s, 3H); 3.85 (s, 3H); ^{13}C NMR (75 MHz, CDCl_3) δ 190.6; 166.2; 162.4; 151.2; 147.2; 131.8; 131.5; 127.9; 123.1; 121.4; 116.9; 113.9; 56.0; 52.3; HRMS (DCI- CH_4) Calculated for $\text{C}_{16}\text{H}_{15}\text{O}_5$ (MH^+): 287.0919. Found: 287.0909.

4.1.2. Synthesis of macrocycle 1

4.1.2.1. Methyl 4-[4-(hydroxymethyl)phenoxy]-3-methoxybenzoate (**8**). To a solution of compound **7** (0.8 g, 2.8 mmol) in a mixture THF/MeOH (1/1, 20 mL) at 4 °C, was added NaBH_4 (0.5 eq). The reaction mixture was stirred for 3 h at room temperature before quenching with saturated aqueous solution of NH_4Cl . The reaction mixture was then concentrated under reduced pressure. The product was extracted with ethyl acetate and the organic phase was washed with H_2O , dried over MgSO_4 , filtered and concentrated in vacuo to afford compound **8** as a white solid upon standing (0.740 mg, 92%). Rf: 0.14 (petroleum ether/ethyl acetate 7/3). ^1H NMR (300 MHz, CDCl_3) δ 7.65 (d, $J = 1.8$ Hz, 1H); 7.58 (dd, $J = 8.2$ Hz, $J = 1.9$ Hz, 1H); 7.32 (m, 2H); 6.97 (m, 2H); 6.85 (d, $J = 8.3$ Hz, 2H); 4.64 (s, 2H); 3.90 (s, 3H); 3.89 (s, 3H); 2.12 (br s, 1H); ^{13}C NMR (75 MHz, CDCl_3) δ 166.6; 155.8; 150.3; 150.1; 136.3; 128.6; 125.6; 123.0; 118.7; 118.3; 113.4; 64.6; 56.0; 52.1; HRMS (DCI- CH_4) Calculated for $\text{C}_{16}\text{H}_{17}\text{O}_5$ (MH^+): 289.1076. Found: 289.1071.

4.1.2.2. ({4-[2-methoxy-4-(methoxycarbonyl)phenoxy]phenyl}methyl)triphenylphosphonium bromide (**9**). Compound **8** (0.800 g, 2.77 mmol) was mixed with triphenylphosphonium bromide (2.77 mmol, 1 eq) in acetonitrile for 4 h and then cooled to room temperature. The reaction mixture was evaporated to afford compound **9** as a white powder which was purified by flash chromatography (gradient ethyl acetate/MeOH 100 to 80/20) to give white powder (1.470 g, 93%). Mp: 101–103 °C. ^1H NMR (300 MHz, CDCl_3) δ 7.66–7.70 (m, 9H); 7.51–7.61 (m, 8H); 7.07 (dd, $J = 8.3$ Hz, $J = 2.7$ Hz, 2H); 6.77 (d, $J = 8.2$ Hz, 1H); 6.70 (d, $J = 8.2$ Hz, 2H); 5.37 (d, $J = 14.1$ Hz, 2H); 3.85 (s, 3H); 3.82 (s, 3H); ^{13}C NMR (75 MHz, CDCl_3) δ 166.3; 156.5 (d, $J = 4.1$ Hz); 150.2; 149.1; 134.9 (d, $J = 2.92$ Hz); 134.2 (d, $J = 9.9$ Hz); 132.9 (d, $J = 5.5$ Hz); 130.1 (d, $J = 12.5$ Hz); 129.9; 126.1; 122.9; 122.1 (d, $J = 8.6$ Hz); 122.0; 118.6; 118.5 (d, $J = 3.2$ Hz); 118.1; 117.0; 113.4; 55.9; 52.1; 29.9 (d, $J = 46.9$ Hz); HRMS (ESI) Calculated for $\text{C}_{34}\text{H}_{30}\text{O}_4\text{P}$ [$\text{M}]^+$: 533.1882. Found: 533.1881.

4.1.2.3. Methyl 4-[4-(2-{4-[4-(5,5-dimethyl-1,3-dioxan-2-yl)-2-methoxyphenoxy]phenyl}ethyl)phenoxy]-3-methoxybenzoate (**13**). The title compound was prepared from compounds **9** and **4**, by following a published procedure [26]. To a solution of phosphonium salt **8** (1.05 eq) in anhydrous dichloromethane (50 mL), were added successively aldehyde **4** (0.690 g, 2.01 mmol, 1 eq), K_2CO_3 (2 eq) and a spatula tip of 18-crown-6. The reaction mixture was stirred for 24 h under reflux and argon. The solution was concentrated in vacuo and the desired product was purified by flash chromatography (gradient petroleum ether/ethyl acetate 9/1 to 5/5). The resulting sticky oil was diluted in AcOEt (8 mL). Palladium on activated carbon (Pd/C 10%, 100 mg/mmol) and triethylamine (1 mL) were added and the resulting solution was stirred for 24 h under H_2 at 0.4 MPa pressure. The mixture was filtered into a filter funnel containing celite. The resulting solution

was evaporated to afford compound **13** as a gummy solid (1.085 g, 90% over two steps). Mp: 127–128 °C. ^1H NMR (300 MHz, CDCl_3) δ 7.66 (d, $J = 1.9$ Hz, 1H); 7.58 (dd, $J = 8.1$ Hz, $J = 1.9$ Hz, 1H); 7.18 (d, $J = 1.8$ Hz, 1H); 7.12 (m, 2H); 7.02–7.07 (m, 3H); 6.92 (m, 2H); 6.81–6.87 (m, 3H); 5.38 (s, 1H); 3.94 (s, 3H); 3.91 (s, 3H); 3.87 (s, 3H); 3.72 (m, 4H); 2.87 (s, 4H); 1.31 (s, 3H); 0.81 (s, 3H); ^{13}C NMR (75 MHz, CDCl_3) δ 166.5; 155.8; 154.2; 151.0; 150.6; 150.0; 145.7; 137.3; 135.7; 134.9; 129.7; 129.3; 125.1; 123.0; 120.2; 118.9; 117.6; 117.3; 113.3; 110.4; 101.3; 77.6; 56.0; 55.9; 52.0; 37.2; 37.1; 30.1; 23.0; 21.8; HRMS (DCI- CH_4) Calculated for $\text{C}_{36}\text{H}_{39}\text{O}_8$ (MH^+): 599.2645. Found: 599.2615.

4.1.2.4. {4-[4-(2-{4-[4-(5,5-dimethyl-1,3-dioxan-2-yl)-2-methoxyphenoxy]phenyl}ethyl)phenoxy]-3-methoxyphenyl}methanol (**14**). To a suspension of lithium aluminium hydride (2 eq) in dry tetrahydrofuran (20 mL) at –40 °C, was added dropwise a solution of compound **13** (0.768 g, 1.28 mmol, 1 eq). The reaction mixture was allowed to warm to room temperature and was stirred for 3 h. Then a saturated aqueous solution of NH_4Cl was added and the resulting mixture was concentrated to give crude oil. The crude oil was dissolved in ethanol and HCl (0.1 N) was added and the mixture was stirred for 2 h at room temperature. After concentration of the solution, the residue was dissolved in AcOEt and the organic phase was washed with water and brine, dried over MgSO_4 , filtered and concentrated. Compound **14** (0.742 g) was directly engaged in the next step without further purification.

4.1.2.5. 4-[4-(2-{4-[4-(hydroxymethyl)-2-methoxyphenoxy]phenyl}ethyl)phenoxy]-3-methoxybenzaldehyde (**15**). Compound **14** (0.742 g, 1.3 mmol) was dissolved in a mixture acetone/ H_2O (20/5 mL) and pyridinium *para*-toluene sulfonate (PPTS, 0.40 eq). The solution was stirred under reflux for 3 h and cooled down. The solution was then concentrated in vacuo to remove acetone and ethyl acetate was added. The organic phase was washed with water and brine, dried over MgSO_4 , filtered and concentrated in vacuo to give colorless oil. The residue was purified by flash chromatography (gradient petroleum ether/ethyl acetate 9/1 to 4/6) to afford compound **15** as a colorless oil (0.474 g, 77% over two steps). Rf: 0.58 (petroleum ether/ethyl acetate: 6/4). ^1H NMR (300 MHz, CDCl_3) δ 9.88 (s, 1H); 7.51 (d, $J = 1.8$ Hz, 1H); 7.36 (dd, $J = 8.1$ Hz, $J = 1.8$ Hz, 1H); 7.15 (m, 2H); 7.08–7.05 (m, 3H); 6.96 (m, 2H); 6.85–6.89 (m, 5H); 4.68 (s, 2H); 3.97 (s, 3H); 3.86 (s, 3H); 2.90 (br s, 4H); ^{13}C NMR (75 MHz, CDCl_3) δ 190.9; 155.9; 153.6; 152.7; 151.3; 150.7; 144.9; 138.0; 137.3; 135.7; 131.9; 130.0; 129.5; 125.8; 120.3; 119.6; 119.4; 117.4; 117; 111.5; 110.5; 65.1; 56.1; 56.0; 37.3; 37.1; HRMS (DCI- CH_4) Calculated for $\text{C}_{30}\text{H}_{28}\text{O}_6$ (M^+): 484.1886. Found: 484.1887.

4.1.2.6. {4-[4-(2-{4-[4-(4-formyl-2-methoxyphenoxy)phenyl]ethyl}phenoxy)-3-methoxyphenyl]methyl}triphenylphosphonium bromide (**16**). The title compound was prepared by following the procedure used for compound **9** and was isolated as white foam (0.760 g, 96%). Rf: 0.53 (dichloromethane/methanol: 9/1). Mp: 119–121 °C. ^1H NMR (300 MHz, CDCl_3) δ 9.86 (s, 1H); 7.71–7.78 (m, 9H); 7.57–7.63 (m, 6H); 7.48 (d, $J = 2.0$ Hz, 1H); 7.34 (dd, $J = 8.3$ Hz, $J = 2.0$ Hz, 1H); 7.11 (d, $J = 8.7$ Hz, 2H); 7.05 (m, 1H); 7.03 (d, $J = 8.7$ Hz, 2H); 6.93 (d, $J = 8.7$ Hz, 2H); 6.84 (d, $J = 8.2$ Hz, 1H); 6.77 (d, $J = 8.5$ Hz, 2H); 6.64 (d, $J = 8.2$ Hz, 1H); 6.55 (dt, $J = 8.2$ Hz, $J = 2.3$ Hz, 1H); 5.42 (d, $J = 14.1$ Hz, 2H); 3.93 (s, 3H); 3.49 (s, 3H); 2.85 (br s, 4H); HRMS (ESI) Calculated for $\text{C}_{48}\text{H}_{42}\text{O}_5\text{P}$ (M^+): 729.2770. Found: 729.2782.

Macrocycle 17. The macrocycle **17** was synthesized in two steps. *First step (cyclization):* Compound **17** (0.250 g, 0.309 mmol) in dry dichloromethane (45 mL) was added over 10 min, to a cold solution of sodium methoxide (8 eq) in dry dichloromethane (100 mL). The mixture was stirred at room temperature for 18 h and was then concentrated under reduced pressure. The product was extracted with ethyl acetate and the organic phase was washed with H_2O , dried over MgSO_4 , filtered and concentrated in vacuo to give a viscous oil which was not

further purified. **Second step (reduction)**: The aforementioned oily product was dissolved in ethyl acetate (10 mL) and palladium on activated carbon (10% Pd, 100 mg/mmol) was added. The resulting suspension was stirred under H₂ at 0.4 MPa pressure for 24 h at room temperature. The reaction mixture was filtered and concentrated to afford a crude oil. The resulting residue was purified by flash chromatography (gradient petroleum ether/ethyl acetate 95/5 to 50/50) to furnish compound **17** as a white oil (0.124 g, 89% over two steps). Rf: 0.65 (petroleum ether/ethyl acetate: 8/2). ¹H NMR (300 MHz, CDCl₃) δ 6.57–6.60 (m, 4H); 6.47–6.51 (m, 6H); 6.41 (d, *J* = 8.1 Hz, 2H); 6.03 (dd, *J* = 8.0 Hz, *J* = 1.8 Hz, 2H); 3.73 (s, 6H); 2.83 (s, 4H); 2.77 (s, 4H); ¹³C NMR (75 MHz, CDCl₃) δ 157.3; 150.4; 145.8; 136.5; 134.9; 130.3; 121.8; 120.0; 118.2; 113.4; 55.9; 37.8; 37.6; HRMS (DCI-CH₄) Calculated for C₃₀H₂₉O₄ (MH⁺): 453.2066. Found: 453.2064.

Macrocyclic M01. To a solution of compound **17** (117 mg, 0.26 mmol), was added BBr₃ (1 M in dichloromethane, 6 eq) at 78 °C. After 2 h30 at this temperature, the reaction mixture was cooled down and stirred for additional 12 h. Cold water was carefully added and the reaction mixture was stirred for 30 min. The solution was diluted with dichloromethane, washed with water then brine, dried over magnesium sulfate and concentrated to afford macrocycle **M01** as a yellow oil. The residue was purified by flash chromatography (gradient petroleum ether/ethyl acetate 9/1 to 5/5) to afford macrocycle **M01** as a lightly yellow solid (0.106 g, 96%). Rf: 0.2 (petroleum ether/ethyl acetate: 8/2). Mp: 177–179 °C. $\nu_{\max}/\text{cm}^{-1}$: 3547; 3410; 3029; 2923; 2855; 1599; 1504; 1334; 1268; 1219; ¹H NMR (300 MHz, CDCl₃) δ 6.68 (d, *J* = 2.1 Hz, 2H); 6.62 (m, 4H); 6.5 (m, 4H); 6.24 (d, *J* = 8.2 Hz, 2H); 5.86 (dd, *J* = 8.1 Hz, *J* = 2.1 Hz, 2H); 5.43 (br s, 2H); 2.79 (s, 4H); 2.77 (s, 4H); ¹³C NMR (75 MHz, CDCl₃) δ 156.8; 147.1; 143.8; 137.2; 135.8; 130.6; 122.2; 118.6; 115.8; 37.7; 37.5; HRMS (ESI) Calculated for C₂₈H₂₃O₄ [M-H]⁺: 423.1596. Found: 423.1595.

CCDC-1958250 (**M01**) contains the supplementary crystallographic data (see supporting information). These data can be obtained free of charge from The Cambridge Crystallographic Data Centre via www.ccdc.cam.ac.uk/data_request/cif.

Selected data for M01: C₂₈H₂₄O₄, 1/2 CH₂Cl₂, *M* = 466.93, monoclinic, space group *P*2₁/*n*, *a* = 19.560(2) Å, *b* = 45.650(5) Å, *c* = 20.292(2) Å, β = 101.668(3)°, *V* = 17745(3) Å³, *Z* = 28, crystal size 0.16 × 0.10 × 0.08 mm³, 243,390 reflections collected (32575 independent, *R*_{int} = 0.2405), 2229 parameters, 197 restraints, *R*₁ [*I* > 2σ(*I*)] = 0.1066, *wR*₂ [all data] = 0.3350, largest diff. peak and hole: 0.577 and −0.507 eÅ^{−3}.

4.1.3. Synthesis of macrocycle M02

4.1.3.1. Methyl 4-(4-formyl-2-methoxyphenoxy)benzoate (10). This compound was synthesized by a similar method (pyridinium *para*-toluenesulfonate, acetone/H₂O, reflux) to that used for the preparation of compound **15**. Compound **10** isolated as a white powder (0.348 g, 83%) was used for the next step without further purification. Rf: 0.58 (petroleum ether/ethyl acetate 6/4). Mp: 115–118 °C. $\nu_{\max}/\text{cm}^{-1}$: 2950; 2920; 1714; 1699; 1612; 1593; 1495; 1283; 1230; ¹H NMR (300 MHz, CDCl₃) δ 9.94 (s, 1H); 8.02 (m, 2H); 7.54 (d, *J* = 1.8 Hz, 1H); 7.46 (dd, *J* = 8.1 Hz, *J* = 1.8 Hz, 1H); 7.11 (d, *J* = 8.1 Hz, 1H); 6.98 (m, 2H); 3.89 (s, 3H); 3.90 (s, 3H); ¹³C NMR (75 MHz, CDCl₃) δ 190.8; 166.4; 160.5; 151.8; 149.7; 133.7; 131.7; 125.5; 125.3; 120.5; 117.3; 111.1; 56.1; 52.1; HRMS (DCI-CH₄) Calculated for C₁₆H₁₅O₅ (MH⁺): 287.0919. Found: 287.0910.

4.1.3.2. Methyl 4-[4-(hydroxymethyl)-2-methoxyphenoxy]benzoate (11) [26]. Compound **11** was synthesized by a similar method to that used for the preparation of compound **8** and was isolated as a colorless oil (0.320 g, 93%). Compound **11** was engaged in the next step without further purification. ¹H NMR (300 MHz, CDCl₃) δ 7.96 (d, *J* = 9.0 Hz, 2H); 7.07 (d, *J* = 1.9 Hz, 1H); 7.07 (d, *J* = 8.1 Hz, 1H); 6.94 (dd, *J* = 8.1 Hz, *J* = 1.9 Hz, 1H); 6.89 (d, *J* = 8.9 Hz, 2H); 4.70 (s, 2H); 3.87 (s, 3H); 3.79 (s, 3H); ¹³C NMR (75 MHz, CDCl₃) 166.7; 162.2;

121.7; 142.6; 139.0; 131.5; 123.8; 122.2; 119.5; 115.7; 11.6; 64.9; 55.8; 51.9; HRMS (DCI-CH₄) Calculated for C₁₆H₁₇O₅ (MH⁺): 289.1076. Found: 289.1069.

4.1.3.3. ({3-Methoxy-4-[4-(methoxycarbonyl)phenoxy]phenyl)methyl}triphenylphosphonium bromide (12) [26]. This compound was synthesized by a similar method to that used for the preparation of compound **9** and it was isolated as a white foam (0.572 g, 79%). The resulting product was used for the next step without further purification. ¹H NMR (300 MHz, CDCl₃) δ 7.94 (m, 2H); 7.75–7.83 (m, 8H); 7.60–7.67 (m, 6H); 7.21 (m, 1H); 6.80 (m, 2H); 6.63 (m, 1H); 5.52 (d, *J* = 13.9 Hz, 2H); 3.87 (s, 3H); 3.47 (s, 3H); HRMS (ESI) Calculated for C₃₄H₃₀O₄P [M]⁺: 533.1882. Found: 533.1879.

4.1.3.4. Methyl 4-[4-(2-[4-[4-(5,5-dimethyl-1,3-dioxan-2-yl)-2-methoxyphenoxy]phenyl]ethyl)-2-methoxyphenoxy]benzoate (18). The title compound was prepared by following the same procedure to that used for the preparation of compound **13** and was purified by flash chromatography (gradient petroleum ether/ethyl acetate 9/1 to 7/3) to furnish compound **18** as a colorless oil (0.471 g, 82% over two steps). ¹H NMR (300 MHz, CDCl₃) δ 7.96 (m, 2H); 7.19 (d, *J* = 1.8 Hz, 1H); 7.03–7.10 (m, 3H); 6.86–6.98 (m, 6H); 6.76–6.79 (m, 2H); 5.39 (s, 1H); 3.89 (s, 3H); 3.88 (s, 3H); 3.79 (d, *J* = 11.1 Hz, 2H); 3.73 (s, 3H); 3.66 (d, *J* = 11.0 Hz, 2H); 2.91 (s, 4H); 1.30 (s, 3H); 0.81 (s, 3H); ¹³C NMR (75 MHz, CDCl₃) δ 166.7; 162.4; 156.0; 151.3; 151.1; 145.7; 141.3; 139.9; 135.6; 135.0; 131.4; 129.4; 123.6; 122.1; 121.0; 120.3; 117.3; 115.6; 113.3; 110.4; 101.4; 77.7; 55.9; 55.8; 51.8; 37.8; 37.1; 30.2; 23.1; 21.8; HRMS (DCI-CH₄) Calculated for C₃₆H₃₉O₈ (MH⁺): 599.2645. Found: 599.2636.

4.1.3.5. {4-[4-(2-[4-[4-(2,2-Dimethyl-1,3-dioxan-5-yl)-2-methoxyphenoxy]phenyl]ethyl)phenoxy]-3-methoxyphenyl}methanol (19). The title compound was prepared from compound **18** (0.468 g, 0.782 mmol), by following the same procedure to that used for the preparation of compound **14**. Compound **19** (0.449 g) was directly engaged in the next step without further purification.

4.1.3.6. 4-[4-(2-[4-[4-(Hydroxymethyl)phenoxy]-3-methoxyphenyl]ethyl)phenoxy]-3-methoxybenzaldehyde (20). The title compound was prepared by following the same procedure to that used for the preparation of compound **15** and was purified by flash chromatography (gradient petroleum ether/ethyl acetate 9/1 in 15 min) to furnish compound **20** as a colorless oil (0.280 g, 74%). ¹H NMR (300 MHz, CDCl₃) δ 9.9(s, 1H); 7.51 (d, *J* = 1.8 Hz, 1H); 7.35 (dd, *J* = 1.8 Hz, *J* = 8.2 Hz, 1H); 7.27 (m, 2H); 7.17 (m, 2H); 6.97 (m, 2H); 6.85–6.91 (m, 4H); 6.76 (d, *J* = 1.8 Hz, 1H); 6.71 (dd, *J* = 7.9 Hz, *J* = 1.8 Hz, 1H); 4.62 (s, 2H); 3.96 (s, 3H); 3.77 (s, 3H); 2.93 (s, 4H); ¹³C NMR (75 MHz, CDCl₃) δ 190.9; 157.7; 153.7; 152.6; 151.1; 150.7; 142.8; 138.5; 137.7; 134.7; 131.9; 129.9; 128.5; 125.7; 121.1; 120.9; 119.5; 117.0; 116.8; 113.2; 110.5; 64.9; 56.1; 55.9; 37.7; 37.2; HRMS (DCI-CH₄) Calculated for C₃₀H₂₈O₆ (M⁺): 484.1886. Found: 484.1874.

4.1.3.7. {4-[4-(2-[4-(4-Formyl-2-methoxyphenoxy)phenyl]ethyl)-2-methoxyphenoxy]phenyl)methyl}triphenylphosphonium bromide (21). The title compound was prepared by following the same procedure to that used for the preparation of compound **9**. Compound **21** was isolated as a colorless foam (0.114 g, 97%). ¹H NMR (300 MHz, CDCl₃) δ 7.67–7.77 (m, 9H); 7.57–7.64 (6H); 7.50 (d, *J* = 1.7 Hz, 1H); 7.35 (dd, *J* = 8.0 Hz, *J* = 1.8 Hz, 1H); 7.15 (d, *J* = 8.6 Hz, 2H); 7.00 (dd, *J* = 8.8 Hz, *J* = 2.7 Hz, 2H); 6.95 (d, *J* = 8.6 Hz, 2H); 6.85 (d, *J* = 8.2 Hz, 1H); 6.81 (d, *J* = 7.8 Hz, 1H); 6.65–6.71 (m, 4H); 5.31 (d, *J* = 13.9 Hz, 2H); 3.95 (s, 3H); 3.73 (s, 3H); HRMS (ESI) Calculated for C₄₈H₄₂O₅P [M]⁺: 729.2770. Found: 729.2766.

Macrocyclic 22. The title compound was prepared by following the same procedure to that used for the preparation of macrocycle **17**. The

resulting residue was purified by flash chromatography (gradient petroleum ether/ethyl acetate 9/1 to 5/5) to afford macrocycle **22** as a white oil (0.112 g, 82% over two steps). ^1H NMR (300 MHz, CDCl_3) δ 6.55 (d, $J = 8.1$ Hz, 2H); 6.52 (br s, 8H); 6.40 (d, $J = 1.8$ Hz, 2H); 6.13 (dd, $J = 8.1$ Hz, 2 Hz, 2H); 3.65 (s, 6H); 2.81 (br s, 8H); ^{13}C NMR (75 MHz, CDCl_3) δ 158.2; 151.4; 144.1; 137.9; 133.8; 129.9; 122.2; 121.9; 116.4; 114.0; 55.9; 38.0; 37.3; HRMS (DCI- CH_4) Calculated for $\text{C}_{30}\text{H}_{29}\text{O}_4$ (MH^+): 453.2066. Found: 453.2067.

Macrocycle M02. The title compound was prepared by following the same procedure than those for macrocycle **M01**. The crude product was purified by flash chromatography (gradient petroleum ether/AcOEt 9/1 to 2/8 in 20 min) to provide macrocycle **M02** as a lightly yellow solid (0.091 g, 88%). Rf: 0.69 (TLC petroleum ether/ethyl acetate 7/3). $\nu_{\text{max}}/\text{cm}^{-1}$: 3442; 3056; 3030; 2925; 2855; 1741; 1596; 1499; 1206; ^1H NMR (300 MHz, MeOD) δ 6.54 (m, 8H); 6.49 (d, $J = 2.0$ Hz, 2H); 6.37 (d, $J = 8.2$ Hz, 2H); 5.83 (dd, $J = 8.2$ Hz, $J = 1.9$ Hz, 2H); 2.75 (m, 8H); ^{13}C NMR (75 MHz, MeOD) δ 159.5; 150.0; 144.5; 139.0; 135.6; 131.1; 123.0; 122.4; 118.3; 117.9; 38.9; 38.3; HRMS (DCI- CH_4) Calculated for $\text{C}_{28}\text{H}_{25}\text{O}_4$ (MH^+): 425.1753. Found: 425.1746.

4.2. Biology

4.2.1. *InhA* activity inhibition

Triclosan and NADH were obtained from Sigma-Aldrich. Stock solutions of all compounds were prepared in DMSO such that the final concentration of this co-solvent was constant at 5% v/v in a final volume of 1 mL for all kinetic reactions. Kinetic assays were performed using *trans*-2-dodecenoyl-coenzyme A (DDCoA) and wild type *InhA* as previously described [37]. Briefly, reactions were performed at 25 °C in an aqueous buffer (30 mM PIPES and 150 mM NaCl pH 6.8) containing additionally 250 μM cofactor (NADH), 50 μM substrate (DDCoA) and the tested compound (at 50 μM or 10 μM). Reactions were initiated by addition of *InhA* (100 nM final) and NADH oxidation was followed at 340 nm. The inhibitory activity of each derivative was expressed as the percentage inhibition of *InhA* activity (initial velocity of the reaction) with respect to the control reaction without inhibitor. Triclosan was used as a positive control. All activity assays were performed in triplicate. For the most potent compounds, IC_{50} values were determined using the 4-parameter curve-fitting software XLFit (IDBS) with at least six points.

4.2.2. MIC determination in *M. tuberculosis* growth inhibition

M. tuberculosis H37Rv was used as the reference strain. *M. tuberculosis* strain was grown at 37 °C in Middlebrook 7H9 broth (Difco), supplemented with 0.05% Tween 80, or on solid Middlebrook 7H11 medium (Difco) supplemented with oleic acid-albumin-dextrose-catalase (OADC). MICs for the new compounds were determined by means of the REMA method [38].

Two independent *M. tuberculosis* cultures were grown approximately to mid-log phase, then diluted to a final $\text{OD}_{600} = 0.0005$ and used to determine MIC in microtiter. Streptomycin and triclosan were used as control. Concentrations assayed were: 40-20-10-5-2.5-1.25-0.6-0.3-0.15 $\mu\text{g}/\text{ml}$, 0 as control. After an incubation of 7 days at 37 °C, resazurin was added at a final concentration of 0.0025%. After 1 day of incubation, plates were read (Ex 544 nm, Em 590 nm, Fluoroskan ThermoScientific).

4.2.3. Molecular docking

Molecular graphics were performed with the UCSF Chimera package [39]. Chimera is developed by the Resource for Biocomputing, Visualization, and Informatics at the University of California, San Francisco (supported by the NIGMS P41-GM103311).

The protein structures used in this paper were structurally aligned with the PDB [40] entry 1BVra [7] (1BVR, chain A) set as reference and using UCSF Chimera/Matchmaker [41] program. The protein structures, in this reference space, were prepared (structure checks,

rotamers, hydrogenation) using Biovia Discovery Studio 2016 (<http://accelrys.com/>) and UCSF Chimera.

The new compounds were sketched using ChemAxon Marvin 16.5, (<http://www.chemaxon.com>). All ligands (extracted from protein structures or new) were checked (hybridization, hydrogenation, some geometry optimizations, 3D sketching) and were merged in SDF libraries using Discovery Studio.

Molecular modeling studies were carried with Molegro Virtual Docker 6 (<http://www.clcbio.com>) software using 1P45a (1P45, chain A) structure [13] as target. A search space (sphere of 15 Å radius) surrounding the binding cavity was used and the ligands were set flexible during the docking. The docking process uses the MolDock [42] function (Moldock [grid] with a resolution of 0.3 Å) for scoring. The Moldock optimizer (6000 iteration steps, population size of 100, 40 independent runs, other parameters let as default) was used for searches. The Tabu clustering was pushed to 1.5 Å (RMSD threshold) in order to increase sensitivity. Post-minimization and post-optimization of H-Bonds parameters were activated; other parameters of this docking protocol were let with default values. No water molecules (entropy penalty) were taken in account in the study [43].

The poses issued from the calculations were ranked, filtered and annotated according to the following sequential rules: {A} the MolDock, Rerank, contributions terms (Interaction, Protein, Cofactor) issued from MolDock calculations were selected to give a table of poses/scores. {B} The table was ranked according to MolDock scores. {C} For all types of scores/contributions, the values were distributed into ranges (as a histogram) of 5 units (giving a scale color in tables). {D} Each pose of the table was compared to others and the poses with the same conformation (in this case a ring topology) were classified. Eventually, a given pose was defined as representative for each topology group. {E} Each pose of interest was manually inspected for the interactions with cofactor NAD, TYR158 and other protein residues. The poses were tagged (+ sign) if a typical network of hydrogen bonds involving TYR158 was possible. {F} The first four best MolDock scores were retained as typical results, and PLANTS [44] score was calculated (re-scoring).

These macrocyclic compounds are relatively rigid molecules; therefore, false positives are known to occur when a full flexibility (softened potentials) scheme is enabled. The protocol takes in account this kind of bias using non flexible (residues) searches. However, after step {E} of protocol, checks were done using a strong minimization (ligand, residues and backbone) in order to ensure that the best pose's conformations do not vary significantly.

The poses were analyzed and compared to different inhibitors co-crystallized in *InhA* structures, particularly the two triclosan residues (TCL500, TC450) found in 1P45a, the c16 fatty acyl substrate (THT) found in 1BVra and the inhibitor PT70 (TCU) found in 2X22a (2X22, chain A) [32] structures.

The poses were classified on the basis of macrocycle topology defined by a letter, a number and a sign. The letter (A or B in this paper) is related to the overall macrocycle envelope in space, the associated number (i.e. A1 or A2) is related to the position of hydroxyl groups (in space). The topologies were tagged (+) if, at least, one hydrogen bond is found possible between the pose and TYR158.

Declaration of Competing Interest

There are no conflicts to declare.

Acknowledgements

The authors are grateful to financial support from the CNRS and the Université Paul Sabatier.

Appendix A. Supplementary material

Supplementary data to this article can be found online at <https://doi.org/10.1016/j.bioorg.2019.103498>.

References

- [1] World Health Organization, Global Tuberculosis Report 2018, World Health Organization, Geneva, Switzerland, 2018.
- [2] E. Pontali, M.C. Raviglione, G.B. Migliori, and the writing group members of the Global TB Network Clinical Trials Committee. Regimens to treat multidrug-resistant tuberculosis: past, present and future perspectives, *Eur. Respir. Rev.* 28 (2019) 190035.
- [3] C. Lange, K. Dheda, D. Chesov, A.M. Mandalakas, Z. Udwadia, C.R. Horsburgh Jr., Management of drug-resistant tuberculosis, *Lancet* 394 (2019) 953–966.
- [4] M. Jankute, J.A. Cox, J. Harrison, G.S. Besra, Assembly of the mycobacterial cell wall, *Annu. Rev. Microbiol.* 69 (2015) 405–423.
- [5] C. Vilchèze, H.R. Morbidoni, T.R. Weisbrod, H. Iwamoto, M. Kuo, J.C. Sacchettini, W.R. Jacobs Jr., Inactivation of the *inhA*-encoded fatty acid synthase II (FASII) enoyl-acyl carrier protein reductase induces accumulation of the FASII end products and cell lysis of *Mycobacterium smegmatis*, *J. Bacteriol.* 182 (2000) 4059–11067.
- [6] A. Quémard, J.C. Sacchettini, A. Dessen, C. Vilchèze, R. Bittman, W.R. Jacobs Jr., J.S. Blanchard, Enzymic characterization of the target for isoniazid in *Mycobacterium tuberculosis*, *Biochemistry* 34 (1995) 8235–8241.
- [7] D.A. Rozwarski, C. Vilchèze, M. Sugantino, R. Bittman, J.C. Sacchettini, Crystal structure of the *Mycobacterium tuberculosis* enoyl-ACP reductase, *InhA*, in complex with NAD⁺ and a C16 fatty acyl substrate, *J. Biol. Chem.* 274 (1999) 15582–15589.
- [8] A. Chollet, L. Mourey, C. Lherbet, A. Delbot, S. Julien, M. Baltas, J. Bernadou, G. Pratiel, L. Maveyraud, V. Bernardes-Génisson, Crystal structure of the enoyl-ACP reductase of *Mycobacterium tuberculosis* (*InhA*) in the apo-form and in complex with the active metabolite of isoniazid pre-formed by a biomimetic approach, *J. Struct. Biol.* 190 (2015) 328–337.
- [9] L.A. Spagnoulo, S. Eltschkner, W. Yu, F. Daryae, S. Davoodi, S.E. Knudsen, E.K. Allen, J. Merino, A. Pschibul, B. Moree, N. Thivalapill, J.J. Truglio, J. Salafsky, R.A. Slayden, C. Kisker, P.J. Tonge, Evaluating the contribution of transition-state destabilization to changes in the residence time of Triazole-based *InhA* inhibitors, *J. Am. Chem. Soc.* 139 (2017) 3417–3429.
- [10] C.W. Levy, A. Roujeinikova, S. Sedelnikova, P.J. Baker, A.R. Stuitje, A.R. Slabas, D.W. Rice, J.B. Rafferty, Molecular basis of triclosan activity, *Nature* 398 (1999) 383–384.
- [11] A. Chollet, G. Mori, C. Menendez, F. Rodriguez, I. Fabing, M.R. Pasca, J. Madacki, J. Kordulakova, P. Constant, A. Quémard, V. Bernardes-Génisson, C. Lherbet, M. Baltas, Design, synthesis and evaluation of new GEQ derivatives as inhibitors of *InhA* enzyme and *Mycobacterium tuberculosis* growth, *Eur. J. Med. Chem.* 101 (2015) 218–235.
- [12] T. Matviuk, F. Rodriguez, N. Saffon, S. Mallet-Ladeira, M. Gorichko, A.L. de Jesus Lopes Ribeiro, M.R. Pasca, C. Lherbet, Z. Voitenko, M. Baltas, Design chemical synthesis of 3-(9H-fluoren-9-yl)pyrrolidine-2,5-dione derivatives and biological activity against enoyl-ACP reductase (*InhA*) and *Mycobacterium tuberculosis*, *Eur. J. Med. Chem.* 70 (2013) 37–48.
- [13] M.R. Kuo, H.R. Morbidoni, D. Alland, D. Alland, S.F. Sneddon, B.B. Gourlie, M.M. Staveski, M. Leonard, J.S. Gregory, A.D. Janjigian, C. Yee, J.M. Musser, B. Kreiswirth, H. Iwamoto, R. Perozzo, W.R. Jacobs Jr., J.C. Sacchettini, D.A. Fidock, Targeting tuberculosis and malaria through inhibition of Enoyl reductase: compound activity and structural data, *J. Biol. Chem.* 278 (2003) 20851–20859.
- [14] T. Matviuk, J. Madacki, G. Mori, B.S. Orena, C. Menendez, A. Kysil, C. André-Barrès, F. Rodriguez, J. Korduláková, S. Mallet-Ladeira, Z. Voitenko, M.R. Pasca, C. Lherbet, M. Baltas, Pyrrolidinone and pyrrolidine derivatives: evaluation as inhibitors of *InhA* and *Mycobacterium tuberculosis*, *Eur. J. Med. Chem.* 123 (2016) 462–475.
- [15] C. Menendez, A. Chollet, F. Rodriguez, C. Inard, M.R. Pasca, C. Lherbet, M. Baltas, Chemical synthesis and biological evaluation of triazole derivatives as inhibitors of *InhA* and antituberculosis agents, *Eur. J. Med. Chem.* 52 (2012) 275–283.
- [16] P.S. Shirude, P. Madhavapeddi, M. Naik, K. Murugan, V. Shinde, R. Nandishaiah, J. Bhat, A. Kumar, S. Hameed, G. Holdgate, G. Davies, H. McMiken, N. Hegde, A. Ambady, J. Venkatraman, M. Panda, B. Bandodkar, V.K. Sambandamurthy, J.A. Read, Methyl-thiazoles: a novel mode of inhibition with the potential to develop novel inhibitors targeting *InhA* in *Mycobacterium tuberculosis*, *J. Med. Chem.* 56 (2013) 8533–8542.
- [17] A. Chollet, L. Maveyraud, C. Lherbet, V. Bernardes-Génisson, An overview on crystal structures of *InhA* protein: apo-form, in complex with its natural ligands and inhibitors, *Eur. J. Med. Chem.* 146 (2018) 318–343.
- [18] R.C. Hartkoorn, F. Pojer, J.A. Read, H. Gingell, J. Neres, O.P. Horlacher, K.H. Altmann, S.T. Cole, Pyridomycin bridges the NADH- and substrate-binding pockets of the enoyl reductase *InhA*, *Nat. Chem. Biol.* 10 (2014) 96–98.
- [19] K. Maeda, H. Kosaka, Y. Okami, H. Umezawa, A new antibiotic, Pyridomycin J. *Antibiot., Ser. A* 6 (1953) 140.
- [20] D.C. Harrowven, S.L. Kostuik, Macrocylic bisbenzyl natural products and their chemical synthesis, *Nat. Prod. Rep.* 29 (2012) 223–242.
- [21] Y.Q. Shi, C.J. Zhu, H.Q. Yuan, B.Q. Li, J. Gao, X.J. Qu, B. Sun, Y.N. Cheng, X. Li, S. Li, H.X. Lou, Marchantin C, a novel microtubule inhibitor from liverwort with anti-tumor activity both in vivo and in vitro, *Cancer Lett.* 276 (2009) 160–170.
- [22] X. Xue, D.F. Sun, C.C. Sun, H.P. Liu, B. Yue, C.R. Zhao, H.X. Lou, X.J. Qu, Inhibitory effect of riccardin D on growth of human non-small cell lung cancer: in vitro and in vivo studies, *Lung Cancer* 76 (2012) 300–308.
- [23] A. Cheng, L. Sun, X. Wu, H. Lou, The inhibitory effect of a macrocyclic bisbenzyl riccardin D on the biofilms of *Candida albicans*, *Biol. Pharm. Bull.* 32 (2009) 1417–1421.
- [24] K. Fujii, D. Morita, K. Onoda, T. Kuroda, H. Miyachi, Minimum structural requirements for cell membrane leakage-mediated anti-MRSA activity of macrocyclic bis(benzyl)s, *Bioorg. Med. Chem. Lett.* 26 (2016) 2324–2327.
- [25] M. Iwashita, S. Fujii, S. Ito, T. Hirano, H. Kagechika, Efficient and diversity-oriented total synthesis of Riccardin C and application to develop novel macrolactam derivatives, *Tetrahedron* 67 (2011) 6073–6082.
- [26] B. Sun, L. Li, Q.-W. Hu, H.-B. Zheng, H. Tang, H.-M. Niu, H.-Q. Yuan, H.-X. Lou, Design, synthesis, biological evaluation and molecular modeling study of novel macrocyclic bisbenzyl analogues as antitubulin agents, *Eur. J. Med. Chem.* 129 (2017) 186–208.
- [27] K. Onada, H. Sawada, D. Morita, K. Fujii, H. Tokiwa, T. Kuroda, H. Miyachi, Anti-MRSA activity of isoplagiochin-type macrocyclic bis(benzyl)s is mediated through cell membrane damage, *Bioorg. Med. Chem.* 23 (2015) 3309–3316.
- [28] A. Dessen, A. Quémard, J.S. Blanchard, W.R. Jacobs, J.C. Sacchettini, Crystal structure and function of the isoniazid target of *Mycobacterium tuberculosis*, *Science* 267 (1995) 1638–1641.
- [29] D.A. Rozwarski, G.A. Grant, D.H. Barton, W.R. Jacobs Jr., J.C. Sacchettini, Modification of the NADH of the isoniazid target (*InhA*) from *Mycobacterium tuberculosis*, *Science* 279 (1998) 98–102.
- [30] T.J. Sullivan, J.J. Truglio, M.E. Boyne, P. Novichenok, X. Zhang, C.F. Stratton, H.J. Li, T. Kaur, A. Amin, F. Johnson, R.A. Slayden, C. Kisker, P.J. Tonge, High affinity *InhA* inhibitors with activity against drug-resistant strains of *Mycobacterium tuberculosis*, *ACS Chem. Biol.* 1 (2006) 43–53.
- [31] J.S. Freundlich, F. Wang, C. Vilchèze, G. Gulsten, R. Langley, G.A. Schiehsler, D.P. Jacobus, W.R. Jacobs, J.C. Sacchettini, Triclosan derivatives: towards potent inhibitors of drug-sensitive and drug-resistant *Mycobacterium tuberculosis*, *ChemMedChem* 4 (2009) 241–248.
- [32] S.R. Luckner, N. Liu, C.W. am, Ende, P.J. Tonge, C. Kisker, A slow, tight binding inhibitor of *InhA*, the enoyl-acyl carrier protein reductase from *Mycobacterium tuberculosis*, *J. Biol. Chem.* 285 (2010) 14330–14337.
- [33] C.T. Lai, H.J. Li, W. Yu, S. Shah, G.R. Bommineni, V. Perrone, M. Garcia-Diaz, P.J. Tonge, C. Simmerling, Rational modulation of the induced-fit conformational change for slow-onset inhibition in *Mycobacterium tuberculosis* *InhA*, *Biochemistry* 54 (2015) 4683–4691.
- [34] H.J. Li, C.T. Lai, P. Pan, W. Yu, N. Liu, G.R. Bommineni, M. Garcia-Diaz, C. Simmerling, P.J. Tonge, A structural and energetic model for the slow-onset inhibition of the *Mycobacterium tuberculosis* enoyl-ACP reductase *InhA*, *ACS Chem. Biol.* 9 (2014) 986–993.
- [35] C.A. Merget, C.A. Sotriffer, Slow-onset inhibition of *Mycobacterium tuberculosis* *InhA*: revealing molecular determinants of residence time by MD simulations, *PLoS One* 10 (2015) 1–25.
- [36] P. Pan, P.J. Tonge, Targeting *InhA*, the FASII Enoyl-ACP reductase: SAR studies on novel inhibitor scaffolds, *Curr. Topics Med. Chem.* 12 (2012) 672–693.
- [37] S.D. Joshi, D. Kumar, S.R. Dixit, N. Tigadi, U.A. More, C. Lherbet, T.M. Aminabhavi, K.S. Yang, Synthesis, characterization and antitubercular activities of novel hydrazones and their Cu-complexes, *Eur. J. Med. Chem.* 121 (2016) 21–39.
- [38] J.C. Palomino, A. Martin, M. Camacho, H. Guerra, J. Swings, F. Portaels, Resazurin microtiter assay plate: simple and inexpensive method for detection of drug resistance in *Mycobacterium tuberculosis*, *Antimicrob. Agents Chemother.* 46 (2002) 2720–2722.
- [39] E.F. Pettersen, T.D. Goddard, C.C. Huang, G.S. Couch, D.M. Greenblatt, E.C. Meng, T.E. Ferrin, UCSF chimera – a visualization system for exploratory research and analysis, *J. Comput. Chem.* 25 (2004) 1605–1612.
- [40] H.M. Berman, J. Westbrook, Z. Feng, G. Gilliland, T.N. Bhat, H. Weissig, I.N. Shindyalov, P.E. Bourne, The protein data bank, *Nucl. Acids Res.* 28 (2000) 235–242.
- [41] E.C. Meng, E.F. Pettersen, G.S. Couch, C.C. Huang, T.E. Ferrin, Tools for integrated sequence-structure analysis with UCSF Chimera, *BMC Bioinform.* 7 (2006) 339–349.
- [42] R. Thomsen, M.H. Christensen, MolDock: a new technique for high-accuracy molecular docking, *J. Med. Chem.* 49 (2006) 3315–3321.
- [43] M.A. Lie, R. Thomsen, C.N.S. Pedersen, B. Schiott, M.H. Christensen, Molecular docking with ligand attached water molecules, *J. Chem. Inf. Model.* 51 (2011) 909–917.
- [44] O. Korb, T. Stütze, T.E. Exner, Empirical scoring functions for advanced protein-ligand docking with PLANTS, *J. Chem. Inf. Model.* 49 (2009) 84–96.